Manganese in the shell of the bivalve *Mytilus edulis*: Seawater Mn or physiological control?

Pedro S. Freitas[a*], Leon J. Clarke[b], Hilary Kennedy[c] and Christopher A. Richardson[c]

a - Divisão de Geologia e Georecursos Marinhos, Instituto Português do Mar e da Atmosfera, Rua Alfredo Magalhães Ramalho, 6, 1495-006 Lisboa, Portugal.

*Corresponding author

e-*mail address*: pedro.freitas@ipma.pt

Phone: +351 21 302 7089

Fax: +351 213 015 948

b - School of Science and the Environment, Faculty of Science and Engineering, Manchester Metropolitan University, Manchester, M1 5GD, United Kingdom

e-*mail address*: l.Clarke@mmu.ac.uk

c - School of Ocean Sciences, College of Natural Sciences, Bangor University, Askew Street, Menai Bridge, LL59 5AB, United Kingdom

e-*mail address*: h.a.kennedy@bangor.ac.uk; c.a.richardson@bangor.ac.uk

Abstract

Manganese in the shell calcite of marine bivalves has been suggested to reflect ambient seawater Mn concentrations, thus providing a high-resolution archive of past seawater Mn concentrations. However, a quantitative relationship between seawater Mn and shell Mn/Ca ratios, as well as clear understanding of which process(es) control(s) shell Mn/Ca, are still lacking. Blue mussels, *Mytilus edulis*, were grown in a one-year duration field experiment in the Menai Strait, U.K., to study the relationship between seawater particulate and dissolved Mn^{2+} concentrations and shell calcite Mn/Ca ratios.

Shell Mn/Ca showed a well-defined intra-annual double-peak, with maximum values during early spring and early summer and low values during autumn and winter. Seawater particulate Mn peaked during winter and autumn, with a series of smaller peaks during spring and summer, whereas dissolved Mn^{2+} exhibited a marked single maximum during late-spring to early-summer, being low during the remainder of the year. Consequently, neither seawater particulate Mn nor dissolved Mn^{2+} concentrations explain the intra-annual variation of shell Mn/Ca ratios.

A physiological control on shell Mn/Ca ratios is evident from the strong similarity and timing of the double-peaked intra-annual variations of Mn/Ca and shell growth rate (SGR), the latter corresponding to periods of increased metabolic activity (as indicated by respiration rate). It is thus likely that in *M. edulis* SGR influences shell Mn/Ca by altering the concentration or activity of Mn^{2+} within the extra-pallial fluid (EPF), by changing the flux of Mn into or the proportion of protein bound Mn within the EPF. By linking shell Mn/Ca ratios to the endogenous and environmental factors that determine growth and metabolic activity, this study helps to explain the lack of a consistent relationship between shell Mn/Ca in marine bivalve shell calcite and seawater particulate and dissolved Mn^{2+} concentrations.

The use of Mn content from *M. edulis* shell calcite as a proxy for the dissolved and/or particulate Mn concentrations, and thus the biogeochemical processes that control them, remains elusive.

1. Introduction

Manganese aquatic geochemistry is dominated by the change between two oxidation states, the soluble Mn^{2+} ion and the insoluble Mn^{4+} ion (e.g. Burton and Statham, 1988), which undergo transformations between the dissolved and particulate phases mainly in response to changes in redox and pH conditions (e.g. Glasby and Schulz, 1999 and references therein). Dissolved Mn^{2+} can be removed from solution by abiogenic oxidation (e.g. Bruland, 1983; Nico et al., 2002), as well as by uptake into or oxide precipitation onto surfaces of bacteria (Emerson et al., 1982; Sunda and Huntsman, 1985; Sunda and Huntsman, 1987) and phytoplankton (Lubbers et al., 1990; Richardson et al., 1988; Richardson and Stolzenbach, 1995; Roitz et al., 2002; Schoemann et al., 1998). Dissolved Mn^{2+} sources include photo-reduction of Mn-oxides, freshwater inputs and release via bacterial reduction of Mn-oxides, particularly from sediments. Bacterial reduction of Mn-oxides occurs when dissolved oxygen concentrations are low and bacteria turn to alternative oxidants for the remineralisation of organic matter, either in sub-oxic micro-environments within suspended aggregates in the water column (Klinkhammer and McManus, 2001) or in the sediments (e.g. Burdige, 1993; Burnett et al., 2003). Benthic and water column fluxes of Mn^{2+} are enhanced in the warmer summer months, as a result of increased biological activity leading to a seasonal input of organic material (e.g. phytoplankton-derived) and lowered oxygen concentrations (Berelson et al., 2003; Dehairs et al., 1989; Hunt, 1983; Sundby et al., 1986). The ability to monitor manganese levels in seawater would thus provide valuable information regarding the environmental processes that control the redox geochemistry of this element in coastal waters.

Bivalves have been shown to be important archives and bio-monitors of environmental conditions (e.g. Richardson, 2001). In particular, the incremental growth of their shell provides a chronologically coherent and high-resolution archive with the capacity to record past changes in the environment in which they lived.

Several studies have indicated the potential of both marine and freshwater bivalve shells as high-resolution time-series recorders of the dissolved and/or particulate Mn concentrations in the water in which the organism grew (Barats et al., 2008; Freitas et

al., 2006; Jeffree et al., 1995; Langlet et al., 2007; Langlet et al., 2006; Lazareth et al., 2003; Lindh et al., 1988; Markich et al., 2002; Poigner et al., 2013; Vander Putten et al., 2000). However, a clear understanding of which process(es) control(s) shell Mn/Ca ratios and development of a quantitative relationship between seawater dissolved and/or particulate Mn and bivalve shell Mn/Ca ratios are still lacking.

For example, aragonitic shells of freshwater unionoid bivalves have been shown to be valid archives of dissolved Mn^{2+} levels associated with riverine anthropogenic inputs (Jeffree et al., 1995; Markich et al., 2002), as well as of both dissolved and biogenic particulate Mn concentrations associated with lacustrine upwelling and associated changes in phytoplankton productivity (Langlet et al., 2007). In marine bivalve shell calcite a similar dichotomy in suggested factors controlling Mn/Ca ratios has been evoked. Seasonal variation of Mn/Ca ratios in the calcitic king scallop *Pecten maximus* (Freitas et al., 2006), has been shown to follow a similar seasonal trend to dissolved Mn^{2+} at the same location (Morris, 1974) suggested to be due to benthic Mn recycling. In addition, Langlet et al. (2006), repeatedly marked oysters (*Cassostrea gigas)* in seawater with artificially elevated dissolved Mn^{2+} concentrations, to produce the first direct evidence for rapid uptake of dissolved Mn^{2+} into the calcite of bivalve shells. In contrast, elevated shell Mn/Ca ratios in *Mytilus edulis* have been suggested to be related to increases in seawater particulate and/or dissolved Mn associated with the sprig bloom (Vander Putten et al., 2000), or increased riverine discharge events for the bivalve *Isognomon ephippium* (Lazareth et al., 2003) and for *P. maximus* (Barats et al., 2008). Constraining the direct influence of either dissolved and/or particulate Mn is difficult and the only studies to have measured both dissolved and particulate Mn concurrently were Langlet et al. (2007) and Barats et al. (2009). In other studies of marine bivalves, seawater particulate and dissolved Mn concentrations have been inferred from changes in other environmental parameters, such as river flow, particulate load or chlorophyll concentrations. Thus far, no study of Mn/Ca shell ratios in a marine bivalve has been made with concurrent measurements of particulate and dissolved Mn concentrations, framed by a well constrained shell chronology.

Given the potential varied control(s) on shell Mn/Ca, a better understanding of the effects and interplay that environmental conditions and physiological processes have

on the incorporation of Mn into bivalve shells is clearly needed before any application of a bivalve shell Mn/Ca palaeoproxy. In this study, specimens of the blue mussel *Mytilus edulis* were grown in a field experiment for a one-year period. The constrained chronology of new shell growth obtained has allowed a novel and reliable comparison to be made, i.e. between shell Mn/Ca ratios and measurements of contemporaneous seawater dissolved and particulate Mn concentrations, shell growth rate and other relevant environmental and physiological variables. Such an approach allows for a realistic and critical assessment of the use of the Mn content of marine bivalve shells as a proxy for seawater dissolved and/or particulate Mn concentrations.

2. Materials and Methods

2.1. Culturing Experiment

The Menai Strait field culturing experiment is described in detail elsewhere (Freitas et al., 2008), with a brief description included here. From 8th December 2004 to 12th December 2005 specimens of the bivalve *M. edulis* were constantly submerged, suspended at 1 metre depth below a moored raft in the Menai Strait, North Wales, U.K. (Fig. 1). The animals were all less than 1-year-old when deployed, obtained from one spat cohort and initially ranged from 2.0 to 2.7 cm in shell length. All individuals used throughout the experiment were selected from a stock of animals, deployed at the beginning of the experiment and kept in a separate cage below the moored raft. Two different, but parallel, experimental approaches were undertaken: 1) "annual"-deployment specimens. Individuals were deployed at the start of the experiment and remained in their own cage for the entire experimental duration (one year). 2) "short"-deployment specimens. Specimens were taken from a stock cage on 16 different occasions, i.e. being in the same physiological condition as their annual-deployment counterparts, were placed into cages for short consecutive periods only, then collected for measurement of physiological variables and sacrificed. Thus combining different individuals allowed a continuous record of growth over the duration (one year) of the field experiment. To establish a constrained growth chronology in both annual- and short-deployment specimens, shell size and thus shell growth was measured at the start and end of 16 consecutive intervals (section 2.4). The duration of each separate growth interval varied between 13 and 52 days, being

dependent on the expected seasonal changes in shell growth rate and in seawater parameters, particularly in dissolved Mn^{2+} concentration.

2.2. Physiological Variables: Shell Growth Rate, Tissue Dry Weight, Condition Index and Respiration Rate

The following specimens were removed from the raft at the end of each experimental growth interval and taken to the laboratory for ca. 6 to 8 hours: all short-deployment *M. edulis* specimens, a new set of short-deployment specimens for the next growth interval and all annual specimens. All shells were handled, photographed and digitally imaged in a similar way (Freitas et al., 2008). To identify and measure all new shell growth for each interval in both short- and annual deployment specimens a combination of shell photographs, shallow hand drilled marks made on the outer shell surface (located away from the margin to avoid disturbing shell growth), and disturbance marks caused by handling were used. In this manner, a well-constrained time control was obtained for the new shell growth deposited throughout the year-long field experiment, by assuming continuous shell growth and a constant shell growth rate during each experimental growth interval.

Condition index (CI) was used to evaluate the proportion of soft tissue relative to the shell (Lucas and Beninger, 1985), as defined by:

CI = tissue dry weight / shell dry weight

At the end of each growth interval, the tissue was removed from short-deployment specimens only, dried to constant weight at 60°C and tissue and shell dry weights measured.

The metabolic rate was measured indirectly from the rate of oxygen consumption (i.e. energy demand; Bayne and Newell, 1983) at the end of each growth interval in short-deployment specimens only. To measure the resting absolute respiration rate (ARR) individual animals were placed into a respirometry chamber kept at ± 0.5°C relative to the water in the Menai Strait. A polarographic dissolved oxygen electrode with automatic temperature compensation and a HiTemp temperature probe (both DCP

Microelements) were used to measure dissolved oxygen and temperature. Calibration to 0 and 100% oxygen saturation was performed using 0.2 µm filtered and U.V. irradiated seawater (FSW) containing dissolved sodium dithionite for 0% saturation and air saturated FSW kept at measurement temperature in a water bath for 100% saturation. A control run was performed before and after each set of measurements to determine blank respiration rates. Animals were allowed to settle in FSW close to oxygen saturation and, after a period of stabilization, the decrease in oxygen saturation was measured for a period between 5 to 30 minutes depending on animal size and seawater temperature. The rate of decrease in oxygen saturation was converted to the rate of oxygen consumption (µmol O_2 h^{-1}) by calculating the amount of oxygen in the chamber. The precision of three replicate measurements of ARR in eight *M. edulis* specimens was better than 7%, expressed as relative standard deviation (RSD). To correct for the dependence of ARR on body size, respiration rates were converted to (soft tissue) weight specific respiration rate (WSRR, µmol O_2 h^{-1} g^{-1}).

2.3. Environmental variables: Seawater Temperature, Salinity, Chlorophyll-a, pH and Nutrient Concentrations

The Menai Strait is a 25 km long shallow channel in the Irish Sea that separates the island of Anglesey from mainland northern Wales, varying in width from a couple of hundred meters to over 5 km. The Menai Strait comprises mainly shallow intertidal mudflats and sand banks, but also includes several rock outcrops, and the water column is completely mixed due to strong turbulent tidal mixing (Harvey, 1968). Several small streams discharge in to the Menai Strait, but the residual water flow from the north-eastern end is dominated by contributions from the Irish Sea, the Conway River and Liverpool Bay (Harvey, 1968; Morris, 1974).

Seawater temperature was monitored every two hours throughout the experimental period using submerged temperature loggers placed in the stock cage (Gemini Data Loggers TinyTag - TGI 3080; accuracy of ± 0.2°C). Seawater samples for the measurements of salinity, chlorophyll-*a*, nutrient concentration (nitrate and nitrite combined, phosphate and silicate), pH and particulate and dissolved Mn^{2+}

concentration were collected every two to five weeks in the vicinity of the moored raft.

Surface seawater samples for salinity measurements were collected using sealed salinity Winchester glass bottles. Salinity was determined using an AutoSal 8400 autosalinometer calibrated with International Association for Physical Sciences of the Ocean (I.A.P.S.O.) standard seawater (analytical accuracy and resolution of ± 0.003 equivalent PSU). For chlorophyll-*a* determinations, a large (10 l) surface seawater sample was collected, agitated to ensure homogeneity and then filtered (500–1000 ml), back in the laboratory, through Whatman GF/C filters (47 mm diameter and nominal pore size 1.2 μm) and frozen for storage. Subsequently, samples were thawed and chlorophyll-*a* and phaeopigments extracted for 18 hours at 4ºC with 90% acetone. Chlorophyll-*a* and phaeopigments were measured using a Turner Design 10-AU fluorometer before and after acidification with 0.1N HCl, respectively (Parsons et al., 1984). Samples for pH measurements were taken by immersing 20 ml plastic syringes below the surface of the seawater. The samples were subsequently allowed to warm up to room temperature (20 ± 2^{o}C), in the dark within the laboratory before measurement (ca. 30 minutes after field collection) with a commercial glass electrode (Mettler Toledo Inlab 412). The electrode was calibrated using NBS pH buffers 6.881 and pH 9.225 (20^{o}C) and was then allowed to stand until a stable reading was obtained (~ 1 min). The filtrates from the chlorophyll-*a* samples were collected in 30 ml clean polythene bottles and kept frozen until subsequent determination of the major dissolved inorganic nutrients. Nitrate and nitrite combined (hereafter termed nitrate), dissolved inorganic phosphorus and silicic acid (hereafter termed silicate), were determined using standard colourimetric methodology (Grasshof et al., 1983), as adapted for flow injection analysis (FIA), on a LACHAT Instruments Quick-Chem 8000 autoanalyzer (Hales et al., 2004).

2.4. Particulate and Dissolved Mn^{2+} Measurements and Mn Partition Coefficient

Particulate Mn was determined following a method adapted from Millward et al. (1998). Samples were collected from the same seawater container used for chlorophyll-*a* sampling and then filtered through 0.4 μm polycarbonate filters of 47 mm diameter, mounted in clean glass filter holders, washed with milli-Q water and

frozen for storage in clean individual petri dishes. After thawing, the filter and the particulate matter were digested in clean centrifuge tubes for 10 hours at room temperature using 1.5 ml of 1M HCl (Aristar grade). This fraction of the particulate Mn represents easily reducible Mn oxides and does not include Mn in detrital mineral grains. Following digestion, samples were centrifuged for one hour to settle the undissolved material and 1 ml of the supernatant diluted between 50 to 400 times depending on Mn concentration. The Mn concentration in the HCl digest solutions was analysed using a Varian Instruments 220Z Zeeman graphite furnace atomic absorption spectrometer, with Zeeman background correction, calibrated using synthetic solutions made up in 1M HCl (Mn concentration range 0–0.273 μmol l^{-1}). Procedure blanks were prepared in the same way by leaching blank filters. Replicate measurements of the digest solution from a particulate Mn sample run concurrently with the samples (0.048 ± 0.002μmol l^{-1}; N = 16) returned an analytical precision of 3.8 % (RSD), while measurements of replicate particulate Mn samples drawn from the same collection bottle (0.045 ± 0.002 μmol l^{-1}; N = 6) showed a sample precision of 3.4 % (RSD).

Samples of surface seawater were collected for determination of dissolved Mn^{2+} using 100 ml polythene syringes. These samples were filtered *in-situ* through an in-line syringe and 0.4 μm polycarbonate filters. The filtrate was collected into a 30 ml HDPE bottle, after discarding the first 10 ml aliquot, and then frozen on return to the laboratory until analysis. Samples were analysed for dissolved Mn concentration using a Varian Instruments 220Z Zeeman graphite furnace atomic absorption spectrometer, with Zeeman background correction, using a method adapted from Su and Huang (1998). A chemical modifier, $Pd(NO_3)_2$, was added to the samples and standards, at a concentration of 2000 μg ml^{-1}, to overcome seawater matrix interferences. Calibration was achieved by standard additions (total Mn concentration range 0.016–0.562 μmol l^{-1}) using 0.2 μm filtered and ultraviolet irradiated Menai Strait seawater. Certified reference seawater (CASS-4, National Research Council, Canada) was analysed with each batch of samples to validate the accuracy of the dissolved Mn measurements. Replicate measurements of CASS-4 (0.053 ± 0.002 μmol l^{-1}; N = 24) returned a recovery of 104.5 % relative to the certified Mn concentration value (0.051 ± 0.003 μmol l^{-1}) and an analytical precision of 4.6 %

(RSD), while the precision of replicate measurements of five seawater samples varied by 4.2 to 12.8 % (RSD).

The relationship between the element composition of a solution and the carbonate precipitating from it is usually described by a non-thermodynamic partition coefficient (e.g. Mucci and Morse, 1990), i.e. $D_E = (E/Ca_{carbonate}) / (E/Ca_{solution})$, where E/Ca are elemental molar ratios. Menai Strait seawater Mn/Ca ratios were calculated from the directly measured dissolved Mn concentration and indirectly Ca concentrations. The latter were calculated from the seawater salinity dataset measured in this study, assuming a Ca concentration of 10.28 mmol kg^{-1} at a salinity of 35 and converted to mmol l^{-1} by correcting for changes in density.

2.5. Shell Preparation and Milling

The left hand valves of *M. edulis* shells obtained from the short- and annual-deployments were cleaned with a brush and the outer organic periostracum was milled away with a hand-held dental drill until periostracum-free shell was visible across the entire sampling area. Calcite shell powder samples then were taken from the shell growth corresponding to each experimental growth interval (see section 2.2.) by milling the outer prismatic layer to a depth of ca. 200 µm using a 0.4 mm wide steel carbide burr (Minerva Dental Ltd). Accurate milling was completed under a binocular microscope fitted with an eyepiece graticule, and depth and width of milling were controlled carefully. Each milled powder sample, ranging in weight from 0.15 to 3.5 mg, was taken from the main axis of shell growth to avoid the increase in shell curvature that occurs away from the main growth axis. Two of the short-deployment specimens (out of the five deployed) were sampled for each experimental growth interval, while three annual-deployment specimens were sequentially sampled for all experimental growth intervals. Sampling resolution was variable depending on the amount of shell growth during each time interval. In both short- and annual-deployment specimens, whenever the amount of shell growth permitted, a single growth interval was divided into equal sequential sub-intervals ($2 \leq N \leq 4$), with each sub-interval providing one sample (sampling resolution is shown in Fig. 3, section 3.3.). Growth was assumed to be continuous and constant during each experimental

growth interval and thus each sub-interval was assumed to represent the same amount of time.

Sampling of seawater variables, with the exception of temperature, occurred at times that corresponded with the start/end of mussel growth intervals and concurrently with the retrieval of short- and annual specimens. In order to perform correlation of shell Mn/Ca with seawater variables, and also to estimate seawater Mn/Ca and the Mn partition coefficient (D_{Mn}), linear interpolation of seawater data at the start and end of each growth interval was used to estimate values for the mid time of each growth interval or sub-intervals.

2.6. Shell Mn/Ca Ratio Analyses

Calibration for shell calcite Mn/Ca ratio determinations was performed via an established ICP-AES intensity-ratio method (de Villiers et al., 2002), using synthetic standard solutions in the range 0.03–0.30 mmol/mol for Mn/Ca ratios, at Ca concentrations of 60 µg ml^{-1}. Sample preparation is described in detail elsewhere (Freitas et al., 2005; Freitas et al., 2006). Measurements were made using a Perkin Elmer Optima 3300RL ICP-AES instrument at the NERC ICP Facility, Royal Holloway University of London. Instrumental drift was monitored by running an intermediate (0.1 mmol/mol) calibration standard every 10 samples and data then were corrected accordingly. Analytical precision (RSD; N = 33) was 4.0 % for Mn/Ca ratios, while replicate measurements of the same milled powder samples obtained from four *M. edulis* specimens showed a sample precision better than 7.5 % RSD. Several shell samples were below Mn detection limits and were excluded from further analysis. For comparison with future datasets, Mn/Ca ratio measurements (± one standard deviation) are reported (Table 1) for three solutions (BAM-RS3, ECRM-752 and CMSI-1767) that have been proposed as certified reference materials (CRMs) for measurement of multi-element /Ca ratios in carbonates (Greaves et al., 2005).Only ECRM-752, however, has a reference value and data from this study contributes to establish reference values for the other two CRMs, BAM-RS3 and CMSI-1767. Replicates were repeated measurements, made on the same ICP-AES instrument as shell Mn/Ca and are of a single dissolution of each CRM, diluted to Ca concentrations of 60 µg ml^{-1} and centrifuged prior to analysis.

Table 1 – Measured Mn/Ca ratios for three multi-element certified reference materials (CRMs) solutions and the available reference value (Greaves et al., 2005).

CRM solution	This study	Reference Value
BAM-RS3	0.011 ± 0.003 (N = 8)	-
ECRM-752	0.141 ± 0.003 (N = 8)	0.15
CMSI-1767	0.075 ± 0.002 (N = 8)	-

3. Results

3.1. Seawater Temperature, Salinity, Chlorophyll-a, pH and Nutrient Concentrations in the Menai Strait

Seawater temperature (Fig. 2a) followed a seasonal change typical of temperate coastal waters, i.e. a winter temperature minimum of ca. 5.0°C at the end of February and a summer temperature maximum of ca. 19.0°C in early–mid July. Salinity in the Menai Strait was lower during winter and early spring, with higher values during late spring and summer, ranging between a minimum of 31.1 to a maximum of 33.6 during the experimental period (Fig. 2b). Chlorophyll-*a* concentration increased from pre-spring bloom values below 1.5 µg l^{-1} at the end of April 2005 to a broad maximum during May 2005 (19.5 µg l^{-1}) that extended over a 5 week period (Fig. 2c). Chlorophyll-*a* then slowly decreased, but remained above pre-bloom values until the end of July, after which concentrations were similar to pre-bloom values throughout the rest of the year. Variation of pH was similar to chlorophyll-*a*, exhibiting maxima from the end of April through to the beginning of June (Fig. 2d). Following a gradual increase from December until April, nutrient concentrations decreased rapidly from mid-April (Fig. 2e). The nitrate (NO_3^- + NO_2^-) and silicate concentrations remained low until September, after which they increased until the end of the year, whereas dissolved inorganic phosphorus concentration increased from June onwards.

3.2. Seawater Particulate and Dissolved Mn Concentrations and Seawater Mn/Ca in the Menai Strait

Seawater particulate Mn concentration (herein after termed Mn_{Part}) showed a marked seasonal variation, with distinct and broad maxima up to ca. 0.18 and ca. 0.14 μmol l^{-1} during January–March and October–November, respectively (Fig. 3a). Lower and variable Mn_{Part}, of 0.01 to 0.11 μmol l^{-1} occurred from April to September. In particular, smaller but still distinct Mn_{Part} maxima occurred during May–July concurrent with the phytoplankton spring bloom.

Seawater dissolved Mn^{2+} concentration (herein after named Mn_{Diss}) seasonal variation was the opposite of Mn_{Part}, being low (<0.06 μmol l^{-1}) from December until the beginning of May and during October–November (Fig. 3a). Mn_{Diss} showed a well-defined maximum of up to 0.54 μmol l^{-1} between early May and early July, followed by a slow decrease to values of ca. 0.09 μmol l^{-1} by early October. The seasonal variation in Mn_{Diss} was similar to the variation of chlorophyll-*a* concentration, in terms of the occurrence of a broad double-peaked maximum, albeit with the maximum Mn_{Diss} lagging the maximum in chlorophyll-*a* concentration by ca. 4 weeks.

Seawater dissolved Mn/Ca was low (<0.01 mmol/mol) from December until the beginning of May and during October–November. As with Mn_{Diss}, a well-defined maximum (up to 0.05 mmol/mol) occurred between early May and early July (Fig. 3b). Variation of seawater dissolved Mn/Ca was clearly controlled by the variation of Mn_{Diss}, therefore only on Mn_{Diss} will be discussed.

3.3. Shell Mn/Ca Records and Mn Partition Coefficient.

In both short- and annual-deployment specimens, shell Mn/Ca ratios showed low values during December to March (usually <0.06 mmol/mol) followed by two clear maxima in April and June (up to 0.19 mmol/mol), with an intermediate minimum (<0.06 mmol/mol) and low values (<0.06 mmol/mol) during the remainder of the year (Fig. 3c). The second Mn/Ca maximum is followed by a sharp decrease at the end of June and two smaller maxima during July (<0.12 mmol/mol). Shell Mn/Ca ratios were significantly correlated, albeit weakly, to SGR and dissolved Mn^{2+} concentration in both short- and annual-deployment specimens (Table 2).

Table 2 – Correlation statistics for shell Mn/Ca ratios with shell growth rate (SGR), dissolved Mn^{2+} concentration (Mn_{Diss}) and seawater Mn/Ca; and correlation statistics for D_{Mn} with Mn_{Diss}, salinity and temperature. r is the pearson correlation coefficient, p is the *p*-value significance probability and N the number of samples.

Shell Mn/Ca	r	*p*	N	**D_{Mn}**	r	*p*	N
		SGR				**Mn_{Dis}**	
All	0.53	<0.001	78		-0.58	<0.001	132
Short	0.51	0.004	30		-0.61	<0.001	58
Annual(all shells)	0.60	<0.001	48		-0.58	<0.001	74
Shell A2	0.57	0.021	16		-0.57	0.004	23
Shell A6	0.69	0.003	16		-0.58	0.004	23
Shell A20	0.67	0.004	16		-0.64	<0.001	28
		Mn_{Diss}				**Salinity**	
All	0.57	<0.001	132		-0.67	<0.001	132
Short	0.60	<0.001	58		-0.73	<0.001	58
Annual(all shells)	0.62	<0.001	74		-0.67	<0.001	74
Shell A2	0.70	<0.001	23		-0.65	0.001	23
Shell A6	0.38	0.077	23		-0.63	0.001	23
Shell A20	0.72	<0.001	28		-0.76	<0.001	28
		Seawater Mn/Ca				**Temperature**	
All	0.57	<0.001	132		-0.77	<0.001	132
Short	0.59	<0.001	58		-0.76	<0.001	58
Annual(all shells)	0.62	<0.001	74		-0.82	<0.001	74
Shell A2	0.70	<0.001	23		-0.85	<0.001	23
Shell A6	0.38	0.077	23		-0.78	<0.001	23
Shell A20	0.72	<0.001	28		-0.86	<0.001	28

The Mn partition coefficient (D_{Mn}) ranged between 0.58 and 26.20, with low values (from 0.58 to 5) from May to October and higher values during winter and autumn (Fig. 3b). D_{Mn} variation was similar and significantly inversely correlated to Mn_{Diss}, salinity and temperature (Fig. 2b and Table 2).

3.4. Soft Tissue Dry Weight, Condition Index, Respiration Rate and Shell Growth Rate

M. edulis soft tissue dry weight (TDW) increased from April until August and the subsequent decrease was likely due to the energy demands of reproductive activities during autumn and winter (Seed and Suchanek, 1992) when availability of food is low (Fig. 4a). Condition Index (CI) was low from December through to the end of March, and then increased in April to maximum values during late May to early July,

reflecting an improvement in energy intake and a net accumulation of soft tissue relative to shell growth (Fig 4a). After July, CI values slowly decreased to low winter values, most likely due to demands from reproductive activities and shell growth. Absolute respiration rate (ARR) increased sharply during April, remaining high through to August, but with a minor drop at the time of the intermediate minima of SGR and Mn/Ca, decreasing afterwards (Fig. 4b). Weight specific respiration rate (WSRR), which compensates for changes in body size, showed two stable periods, the first with higher values between December to March and the second with lower values from August until December (Fig. 4b). In between these stable periods, WSSR showed a decreasing trend, but with two clear maxima during April and June. Shell growth rate (SGR) was lowest during December (ca. 50 μm day^{-1}), increasing until the end of June, with two clear maxima in April and June (up to 200 and 400 50 μm day^{-1}, respectively), and then decreased steadily to low values until December (Fig. 4c). The pattern of SGR variation of both short- and annual-deployment specimens was similar.

4. Discussion

4.1. Variation of Particulate and Dissolved Mn Concentrations within the Menai Strait

In the coastal and estuarine waters of the North Sea, high winter Mn_{Part} has been shown to be associated with high winter suspended particulate matter (SPM) loads, attributed to sediment resuspension by seasonally-elevated wind speeds and larger swell (Dellwig et al., 2007; Turner and Millward, 2000). In this study, Mn_{Part} maxima (Fig. 3a), occur at a similar time to expected high SPM (Buchan et al., 1973; Kratzer et al., 2003), dominated by inorganic particles re-suspended from the seabed (Kratzer et al., 2000; Kratzer et al., 2003). The concurrent low Mn_{Diss} concentration (Fig. 3a) most likely resulted from significant removal into oxide coatings on SPM and sediments grains (e.g. Bruland, 1983; Burton and Statham, 1988) alongside low seawater temperatures and well-mixed and well-oxygenated water column (e.g. Burdige, 1993; Burnett et al., 2003). The influence of freshwater inputs on Mn_{Diss} was

likely negligible, as suggested by the small variation in salinity in the Menai Strait during 2005 (Fig. 2b), a conclusion also drawn by Morris (1974).

During spring and summer, Mn_{Part} and Mn_{Diss} (Fig. 3a) were marked by: 1) a reduction in Mn_{Part}, likely via a decrease in the SPM load (Morris, 1974) and from the reduction of Mn-oxides in SPM (Morris, 1971); 2) a broad increase in Mn_{Diss}. The variation in Mn_{Diss} is similar to that described by Morris (1974) who concluded that it was the result of increased benthic fluxes of Mn^{2+}.

In this study, Mn_{Diss} increased markedly during the spring bloom (Fig. 3a), as defined by the increase in chlorophyll-*a* and a decrease in nutrient concentrations (Fig. 2c, d, e). Peak Mn_{Diss} values occurred after the period of highest primary production (Fig. 2c), when chlorophyll-*a* concentration decreased, in a pattern often observed in coastal waters (Schoemann et al., 1998). The time of peak Mn_{Diss} (early June) is that of the expected increase in heterotrophic activity in the water column of the Menai Strait, (Blight et al., 1995). Bloom-derived, organic-rich suspended aggregates provide the conditions in the water column for sub-oxic micro-environments to develop, increasing the reduction of Mn_{Part} and release of Mn^{2+} into solution (e.g. Klinkhammer and McManus, 2001). Peak Mn_{Diss} also coincided with a late-bloom increase in dissolved inorganic phosphorus concentration (Figs. 2e and 3a), which is indicative of high organic matter remineralisation in the water column or in the sub-oxic/anoxic conditions in the sediments, both of which strongly favour the release of Mn^{2+} (Kowalski et al., 2012). Therefore, the main factor determining the broad Mn_{Diss} maximum (Fig. 3a) likely was the production and release of Mn^{2+} associated with raised heterotrophic activity and organic matter remineralisation in the water column and sediments during the warmer spring–summer months (Kowalski et al., 2012).

The short-lived concurrent increases and decreases in Mn_{Part} and Mn_{Diss} (Fig. 3a), respectively, during the spring bloom from April to July are most likely the result of Other factors controlling both reduction and adsorption of Mn_{Part} and remobilisation of Mn_{Diss} over shorter time scales. For instance, surface adsorption of Mn^{2+} to *Phaeocystis sp.* bladder colonies and diatoms may increase Mn_{Part} during bloom conditions in coastal waters (Davidson and Marchant, 1997; Lubbers et al., 1990; Morris, 1974; Schoemann et al., 1998).

4.2. Shell Mn/Ca ratios in Mytilus edulis, Dissolved and Particulate Mn, and D_{Mn}

Shell Mn/Ca ratios measured in *M. edulis* in this study (Fig. 3c) were generally of the same order of magnitude as those reported for marine bivalve calcite and differed from those previously observed only in a few instances. Shell Mn/Ca ratios were three to four times lower than in laboratory cultured *M. edulis* (Freitas et al., 2009), about half the values observed in *M. edulis* from the Scheldt estuary, Netherlands (Vander Putten et al., 2000) and about 10 times higher than in *P. maximus* from the Bay of Brest, France (Barats et al., 2009). In our particular study site, *P. maximus* grown during 1994–1995 (Freitas et al., 2006) displayed similar values to *M. edulis* (Fig. 3c), but only had a single broad maximum during spring and early summer.

There is no consensus whether direct uptake of dissolved Mn^{2+} (e.g. Barbin et al., 2008; Freitas et al., 2006; Langlet et al., 2006) or particulate Mn by bivalves act as sources of Mn to bivalve shells (e.g. Barats et al., 2008; Carriker et al., 1980; Langlet et al., 2007; Lazareth et al., 2003; Vander Putten et al., 2000).

In this study, *M. edulis* shell Mn/Ca showed a markedly different intra-annual variation than both seawater Mn_{Part} and Mn_{Diss} or seawater Mn/Ca (Fig. 3), and was not significantly related to Mn_{Part} and only weakly related to Mn_{Diss} (Table 2). A clear disparity between shell Mn/Ca and seawater Mn_{Part} and Mn_{Diss} is obvious during the first Mn/Ca maximum and the subsequent intermediate Mn/Ca minimum. Paradoxically, the first Mn/Ca maximum occurs at a time when Mn_{Diss} and Mn_{Part} are at their lowest, while the intermediate Mn/Ca minimum occurs at a time when Mn_{Diss} is readily available and Mn_{Part} availability is likely increased from preferential sorting for high-quality, organic-rich and Mn enriched particles, which has been shown to lead to enhanced Mn uptake in mussels (Widmeyer et al., 2004).

In contrast, shell Mn/Ca and seawater Mn_{Diss} peaks showed a good temporal overlap during the second Mn/Ca maximum (Fig. 3) and thus suggest that shell Mn/Ca may have increased in response to the increase in Mn_{Diss} concentration. However, shell Mn/Ca increased fairly abruptly and lagged the increase in Mn_{Diss} by about two to

three weeks, whereas the later decrease of Mn/Ca and Mn_{Diss} occurred concurrently (Fig. 3).

D_{Mn} in *M. edulis* (Fig. 3b) was similar to the range observed in experimentally precipitated inorganic calcite (Droomgoole and Walter, 1990). However, while the latter was shown to have a positive dependence on temperature (Droomgoole and Walter, 1990), D_{Mn} in *M. edulis* was inversely related both to salinity and temperature (Fig. 3 and Table 2) and thus suggest different controls on the partitioning between bivalve calcite and Mn_{Diss} compared to abiogenic calcites. Partition coefficients do not take into account the activity coefficients of ions in solution, nor that in bivalves the shell carbonate is formed from a solution (i.e. the extra-pallial fluid or EFP) isolated from seawater.

In bivalves, transportation of dissolved Mn^{2+} from seawater to the shell is expected to be fast. Marking experiments using concentrations two to four orders of magnitude higher than in natural waters showed that uptake of dissolved Mn took only a few days in freshwater mussels (Jeffree et al., 1995) to 30 minutes to less than 24hours in marine oysters (Barbin et al., 2008; Langlet et al., 2006; Lartaud et al., 2010) and a few days at most in *P. maximus* (Barats et al., 2009). In this study there was a two to three weeks lag between the increase of seawater Mn_{Diss} and shell Mn/Ca (Fig. 3), which could be explained by a Mn_{Diss} concentration threshold, below which shell Mn/Ca ratios do not respond to changes in Mn_{Diss} concentrations. If early June is taken as the start of the shell Mn/Ca peak and early July as its end, a threshold concentration ca. 0.30 µmol l^{-1} can be deduced for *M. edulis* in this study (Fig. 3).

In summary, the seasonal variation in shell Mn/Ca cannot be explained by either seawater Mn_{Part} or Mn_{Diss} and no single mechanism can explain the two shell Mn/Ca maxima, which were likely determined by different processes.

4.3. A Physiological Control of Shell Mn/Ca in Mytilus edulis?

The lack of a clear relationship between *M. edulis* shell Mn/Ca and seawater Mn_{Part} or Mn_{Diss} suggests a control by other factors, most likely physiological or kinetic in

origin. This suggestion is supported by the seasonal variations of soft tissue size, physiological condition, shell growth rate and metabolic activity (Fig. 4a, b, c). The seasonal variation of shell growth rates (SGR) in *M. edulis* (Fig. 4c) was strikingly similar ($0.51 < r < 0.68$, $p < 0.001$; Table 2) to the seasonal variation of shell Mn/Ca (Fig. 4d). Significant relationships between SGR and Mn/Ca in bivalve calcite have not been observed in studies that investigated other species at this study site (Freitas et al., 2006) or the same species at other locations (Barats et al., 2008). In bivalves, a significant relationship between growth rate and Mn/Ca ratios has been only reported in two marine aragonitic species from South America, *Mesodesma donacium* and *Chione subrugosa* (Carré et al., 2006). Synthetic inorganic calcite precipitation experiments have clearly shown an inverse relationship between precipitation rate and the Mn partition coefficient (Dromgoole and Walter, 1990; Lorens, 1981; Mucci, 1988; Pingitore et al., 1988). Therefore, the similarity between the seasonal variation of SGR and shell Mn/Ca in *M. edulis* does not appear to be indicative of a kinetic calcite precipitation rate control, but must reflect other processes, likely physiological in origin.

In bivalves, shell carbonate is not precipitated from ambient water, but from the extra-pallial fluid (EPF) (Wilbur and Saleuddin, 1983), located between the mantle and the inner shell surface. The EPF is an isolated solution with a different chemical composition to that of the external medium, with both the external medium and animal tissues supplying elements to the EPF (Crenshaw, 1972; Pietrzak et al., 1976; Wada and Fujinuki, 1976; Wilbur and Saleuddin, 1983). In bivalves, and in *M. edulis*, divalent metals can be stored in a variety of reservoirs, e,g, bound to proteins present in soft tissue, haemolymph and also in the EPF or in polymetalic granules within the kidney, digestive gland, mantle or gills (Carmichael et al., 1980; Marigómez et al., 2002; Park et al., 2009; Pentreath, 1973; Simkiss and Mason, 1984; Wang and Rainbow, 2008; Yin et al., 2005).

In the marine mussel *M. edulis*, only a small fraction of the Mn in the EPF is present as free ionic Mn, with the majority bound to organic molecules (Misogianes and Chasteen, 1979). The main protein component of the EPF of *M. edulis* was found to closely resemble a heavy metal binding protein from the haemolymph and to bind divalent ions other than Ca^{2+}, including Mn^{2+} (Yin et al., 2005). This protein was

suggested to also function as a precursor to, or a building block of, the soluble organic matrix of the shell (Hattan et al., 2001). It is thus likely that a physiological control of the Mn content of the EPF in *M. edulis* involves the main protein component of the EPF and may ultimately influence the Mn content of the shell. Importantly, Wada and Fujinuki (1976) found that Mn/Ca ratios in the inner EPF of four marine bivalve species (not *M. edulis*) was higher during periods of increased growth than during periods of reduced growth.

If the observations described above are applicable to the outer EPF of *M. edulis*, where shell deposition at the margin occurs, a physiological control can be conceived by which SGR influences the concentration and/or activity of Mn (hereafter referred to as Mn content) in the EPF, which in turn will influence shell Mn/Ca ratios. Under such physiological control, high rates of shell deposition would increase the EPF Mn content and ultimately cause higher shell Mn/Ca ratios, while the reverse would occur at low SGR, i.e. a decrease in the EPF Mn content leading to reduced shell Mn/Ca ratios. The physiological control described above is further supported by the model proposed by Carré et al. (2006) for trace metal incorporation, including Mn, into bivalve aragonite. In their model, active ion transport to the EPF mediated by Ca-channels would determine trace metal transport to the EPF (Carré et al., 2006). Since the ion selectivity of Ca-channels decreases with increasing ion flux, i.e. with growth rate, trace element transport to the EPF relative to calcium increases at higher growth rates.

Therefore, SGR could influence the EPF Mn content by changing the flux of Mn into the EPF, either from the external medium or from internal reservoirs, but also by affecting protein-bound Mn in the EPF, e.g. high mineralization rates would induce the release in the EPF of free ionic Mn^{2+} from protein-bound Mn, with the reverse occurring at low mineralization rates. Additionally, the incorporation into the shell organic matrix of protein-bound Mn from the EPF cannot be discarded and may also affect shell Mn/Ca ratios.

The intermediate minima in SGR and metabolic activity (Fig. 4b, c) results from a reduction in feeding. Large *Phaeocystis sp.* colonies, which occur in the Menai Strait during the peak of the spring bloom (Blight et al., 1995; Morris, 1971), are known to

cause clogging of the gills and reduced food intake and digestion in *M. edulis* (Pieters et al., 1980; Prins et al., 1994; Smaal and Twisk, 1997) and consequently a decrease in energy intake at this time likely led to a reduction in metabolic activity and to energy use being diverted away from shell growth to sustain tissue growth and reproductive activities (Seed and Suchanek, 1992; Small et al., 1997).

Under the proposed physiological control, increased SGR during the first shell Mn/Ca maximum (Fig. 4b, c, d), driven by higher metabolic activity, would drive higher transport of Mn into the EPF increasing its Mn content. Mn would likely come from the remobilization of internal reservoirs in *M. edulis*, since seawater Mn_{Part} and Mn_{Diss} were low at that time (Fig. 3). The distinct shell Mn/Ca minimum could not result from a lack of Mn in the environment, which was readily available either as Mn_{Part} or Mn_{Diss} (Fig. 3). Therefore, it can be hypothesized that shell Mn/Ca ratios in *M. edulis* were modulated by changes in SGR, itself driven by changes in metabolic activity and energy uptake and allocation, which in turn determined the Mn content of the EPF and thus its availability for incorporation into shell carbonate.

The physiological control of bivalve shell Mn/Ca proposed here for *M. edulis* exposes shell Mn/Ca to the influence of the endogenous and environmental factors that determine growth and metabolic activity, e.g. size, age, and physiological condition, activity level, food availability and temperature (e.g. Bayne and Newell, 1983; Gosling, 2003). Therefore, the degree of physiological control of bivalve shell Mn/Ca can be expected to vary in different species, but also within the same species, e.g. different age and/or environmental conditions during growth. In particular, the degree of physiological control of shell Mn/Ca will depend on the proportion of Mn in the EPF that derives from the external medium or internal reservoirs in each species. That proportion will be determined by the degree of isolation of the EPF, which in bivalves is species-specific (Harper, 1997). Nevertheless, the proposed physiological control of shell Mn/Ca can explain, at least partially, the lack of a consistent relationship between shell Mn/Ca in marine bivalve calcite and seawater particulate and dissolved Mn concentrations.

5. Conclusions

Neither seawater particulate Mn nor dissolved Mn^{2+} concentrations could explain the measured seasonal variation in *M. edulis* shell calcite Mn/Ca ratios. A physiological control of shell Mn/Ca ratios in *M. edulis* is strongly supported by the high degree of similarity between the intra-annual variations of shell Mn/Ca and shell growth rates, the latter driven by changes in metabolic activity and energy uptake and allocation. A physiological control is proposed whereby shell growth rates influence *M. edulis* shell Mn/Ca ratios by determining the concentration and/or activity of Mn in the EPF and thus its availability for incorporation within shell carbonate. Shell growth rate would act by affecting the flux of Mn into the EPF, either from the external medium or from internal reservoirs, or the release of protein-bound Mn into the EPF. Use of the Mn content of *Mytilus edulis* shell calcite as a proxy for seawater dissolved and/or particulate Mn concentrations, and thus the biogeochemical processes that control these parameters, is unlikely.

Acknowledgements

The authors thank Berwyn Roberts and Gwynne Jones Hughes for their technical support with the field experiment. Access to the then U.K. Natural Environment Research Council ICP-AES Facility at Royal Holloway University of London, award No. OSS/273/1104, as well as the technical assistance of Nick Walsh and Emma Tomlinson is acknowledged gratefully. This research was partially funded by Fundação para a Ciência e Tecnologia (FCT), Portugal, through a grant to Pedro Freitas, Contract No. SFRH/BD/10370/2002.

References

Barats A., Amouroux D., Chauvaud L., Pécheyran C., Lorrain A., Thebault J., Church T. and Donard O. (2009) High frequency Barium profiles in shells of the Great Scallop *Pecten maximus*: a methodical long-term and multi-site survey in Western Europe. *Biogeosciences* **6**, 157-170.

Barats A., Amouroux D., Pécheyran C., Chauvaud L. and Donard O. F. X. (2008) High-Frequency Archives of Manganese Inputs To Coastal Waters (Bay of Seine, France) Resolved by the LA-ICP-MS Analysis of Calcitic Growth Layers along Scallop Shells (*Pecten maximus*). *Environ. Sci. Technol.* **42**, 86-92.

Barbin V., Ramseyer K. and Elfman M. (2008) Biological record of added manganese in seawater: a new efficient tool to mark in vivo growth lines in the oyster species *Crassostrea gigas*. *Int. J. Earth Sci.* **97**, 193-199.

Bayne B. and Newell R. (1983) Physiological energetics of marine molluscs. In *The Mollusca* (eds. A. S. M. Saleuddin and K. M. Wilbur). Academic Press, New York. pp. 407-515.

Berelson W., MacManus J., Coale K., Johnson K., Burdige D., Kilgore T., Colodner D., Chavez F., Kudela R. and Boucher J. (2003) A time series of benthic flux measurements from Monterey Bay, CA. *Cont. Shelf Res.* **23**, 457-481.

Blight S., Bentley T., Lefevre D., Robinson C., Rodrigues R., Rowlands J. and Williams P. (1995) Phasing of autotrophic and heterotrophic plankton metabolism in a temperature coastal ecosystem. *Mar. Ecol. Prog. Ser.* **128**, 61-75.

Bruland K. (1983) Trace elements in sea water. In *Chemical Oceanography* (ed. R. Chester). Academic Press, London. pp. 157-220.

Buchan S., Floodgate G. and Crisp D. (1973) Studies of the seasonal variation of the suspended matter of the Menai Straits II. Mid stream data. *Ocean Dynam.* **26**, 74-83.

Burdige D. (1993) The biogeochemistry of manganese and iron reduction in marine sediments. *Earth Sci. Rev.* **35**, 249-284.

Burnett W., Bokuniewicz H., Huttel M., Moor W. and Taniguchi M. (2003) Groundwater and pore water inputs to the coastal zone. *Biogeochemistry* **66**, 3-33.

Burton J. and Statham P. (1988) Trace Metals as Tracers in the Ocean. *Phil. Trans. R. Soc. London, Series A* **325**, 127-144.

Carmichael N. G., Squibb K. S., Engel D. W. and Fowler B. A. (1980) Metals in the molluscan kidney: Uptake and subcellular distribution of ^{109}Cd, ^{54}Mn and ^{65}Zn by the clam, *Mercenaria mercenaria*. *Comp. Biochem. Phys. A* **65**, 203-206.

Carré M., Bentaleb I., Ordinola E. and Fontugne M. (2006) Calcification rate influence on trace elements incorporation in marine bivalve aragonite: evidences and mechanisms. *Geochim. Cosmochim. Ac.* **70**, 4906-4920.

Carriker M. R., Palmer R. E., Sick L. V. and Johnson C. C. (1980) Interaction of mineral elements in sea water and shell of oysters (*Crassostrea virginica* (Gmelin)) cultured in controlled and natural systems. *J. Exp. Mar. Biol. Ecol.* **46**, 279-296.

Crenshaw M. (1972) The inorganic composition of molluscan extrapallial fluid. *Biol. Bull.* **143**, 505-512.

Davidson A. and Marchant H. (1987) Binding of manganese by Antartic *Phaeocystis pouchetii* and the role of bacteria in its release. *Mar. Biol.* **95**, 481-487.

de Villiers S., Greaves M. and Elderfield H. (2002) An intensity ratio calibration method for the accurate determination of Mg/Ca and Sr/Ca of marine carbonates by ICP-AES. *Geochem. Geophy. Geosy.* **3**, 1001,1010.1029/2001GC000169.

Dehairs F., Baeyens W. and Van Gansbeke D. (1989) Tight coupling between enrichment of iron and manganese in North Sea suspended matter and sedimentary redox processes: Evidence for seasonal variability. *Estuar. Coast. Shelf S.* **29**, 457-471.

Dellwig O., Bosselmann K., Kolsch S., Hentscher M., Hinrichs J., Bottcher M., Reuter R. and Brumsack H. (2007) Sources and fate of manganese in a tidal basin of the German Wadden Sea. *J. Sea Res.* **57**, 1-18.

Dromgoole E. and Walter L. (1990) Iron and manganese incorporation into calcite: effects of growth kinetics, temperature and solution chemistry. *Chem. Geol.* **81**, 311-336.

Emerson S., Kalhorn S., Jacobs S., Tebo B., Nealson K. and Rosson R. (1982) Environmental oxidation rate of manganese(II): bacterial catalysis. *Geochim. Cosmochim. Ac.* **46**, 1073-1079.

Freitas P., Clarke L., Kennedy H., Richardson C. A. and Abrantes F. (2005) Mg/Ca, Sr/Ca and stable-isotope ($\delta^{18}O$ and $\delta^{13}C$) ratio profiles from the fan mussel *Pinna nobilis*: Seasonal records and temperature relationships. *Geochem. Geophy. Geosy.* **6**, Q04D14, doi:10.1029/2004GC000872.

Freitas P. S., Clarke L. J., Kennedy H. and Richardson C. A. (2009) Ion microprobe assessment of the heterogeneity of Mg/Ca, Sr/Ca and Mn/Ca ratios in *Pecten maximus* and *Mytilus edulis* (bivalvia) shell calcite precipitated at constant temperature. *Biogeosciences* **6**, 1209-1227.

Freitas P. S., Clarke L. J., Kennedy H., Richardson C. A. and Abrantes F. (2006) Environmental and biological controls on elemental (Mg/Ca, Sr/Ca and Mn/Ca) ratios in shells of the king scallop *Pecten maximus*. *Geochim. Cosmochim. Ac.* **70**, 5119-5133.

Freitas P. S., Clarke L. J., Kennedy H. A. and Richardson C. A. (2008) Inter- and intra-specimen variability masks reliable temperature control on shell Mg/Ca ratios in laboratory- and field-cultured *Mytilus edulis* and *Pecten maximus* (bivalvia). *Biogeosciences* **5**, 1245-1258.

Glasby G. P. and Schulz H. (1999) E_H, pH diagrams for Mn, Fe, Co, Ni, Cu and As under seawater conditions: application of two new types of E_H, pH diagrams to the study of specific problems in marine geochemistry. *Aquat. Geochem.* **5**, 227-248.

Gosling E. (2003) *Bivalve Molluscs: Biology, Ecology and Culture*. Blackwell Scientific Publications, Oxford.

Grasshof K., Wehrhardt M. and Kremling K. (1983) Methods of Seawater Analysis. 2nd ed. Verlag Chemie, Weinheim.

Greaves M., Barker S., Daunt C. and Elderfield H. (2005) Accuracy, standardization, and interlaboratory calibration standards for foraminiferal Mg/Ca thermometry. *Geochem. Geophy. Geosy.* **6**, Q02D13, doi:10.1029/2004GC000790.

Hales B., van Geen A. and Takahashi T. (2004) High-frequency measurement of seawater chemistry: Flow-injection analysis of macronutrients. *Limnol. Oceanogr.-Meth.* **2**, 91-101.

Harper E. (1997) The molluscan periostracum: an important constraint in bivalve evolution. *Palaeontology* **40**, 71-97.

Harvey J. (1968) The flow of water through the Menai Strait. *Geophys. J. Roy. Astr. S.* **15**, 517-528.

Hattan S. J., Laue T. M. and Chasteen N. D. (2001) Purification and characterization of a novel calcium-binding protein from the extrapallial fluid of the mollusc *Mytilus edulis*. *J. Biol. Chem.* **276**, 4461-4468.

Hunt C. (1983) Variability in the benthic Mn flux in coastal marine ecosystems resulting from temperature and primary production. *Limnol. Oceanogr.* **28**, 913-923.

Jeffree R., Markich S., Lefebvre F., Thellier M. and Ripoll C. (1995) Shell microlaminations of the fresh-water bivalve *Hyridella depressa* as an archival monitor of manganese concentration: Experimental investigation by depth profiling using secondary-ion mass-spectrometry (SIMS). *Experientia* **51**, 838-848.

Klinkhammer G. and McManus J. (2001) Dissolved manganese in the Columbia River estuary: Production in the water column. *Geochim. Cosmochim. Ac.* **65**, 2835-2841.

Kowalski N., Dellwig O., Beck M., Grunwald M., Durselen C.-D., Badewien T. H., Brumsack H.-J., van Beusekom J. E. E. and Bottcher M. E. (2012) A comparative study of manganese dynamics in the water column and sediments of intertidal systems of the North Sea. *Estuar. Coast. Shelf S.* **100**, 3-17.

Kratzer S., Bowers D. and Tett P. (2000) Seasonal changes in colour ratios and optically active constituents in the optical case-2 waters of the Menai Strait, North Wales. *Int. J. Remote Sens.* **21**, 2225-2246.

Kratzer S., Buchan S. and Bowers D. (2003) Testing long-term trends in turbidity in the Menai Strait, North Wales. *Estuar. Coast. Shelf S.* **56**, 221-226.

Langlet D., Alleman L., Plisnier P.-D., Hughes H. and André L. (2007) Manganese content records seasonal upwelling in Lake Tanganyika mussels. *Biogeosciences* **4**, 195-203.

Langlet D., Alunno-Bruscia M., Rafelis M., Renard M., Roux M., Schein E. and Buestel D. (2006) Experimental and natural cathodoluminescence in the shell of *Crassostrea gigas* from Thau lagoon (France): ecological and environmental implications. *Mar. Ecol. Prog. Ser.* **317**, 143-156.

Lartaud F., de Rafelis M., Ropert M., Emmanuel L., Geairon P. and Renard M. (2010) Mn labelling of living oysters: Artificial and natural cathodoluminescence analyses as a tool for age and growth rate determination of *Cassostrea gigas* (Thunberg, 1793) shells. *Aquaculture* **300**, 206-217.

Lazareth C. E., Vander Putten E., Andre L. and Dehairs F. (2003) High-resolution trace element profiles in shells of the mangrove bivalve *Isognomon ephippium*: a record of environmental spatio-temporal variations? *Estuar. Coast. Shelf S.* **57**, 1103-1114.

Lindh U., Mutvei H., Sunde T. and Westermark T. (1988) Environmental history told by mussel shells. *Nucl. Intrum. Meth. B* **30**, 388-392.

Lorens R. (1981) Sr, Cd, Mn and Co distribution coefficients in calcite as a function of calcite precipitation rate. *Geochim. Cosmochim. Ac.* **45**, 553-561.

Lubbers G., Giesles W., del Castillo P., Salomons W. and Bril J. (1990) Manganese accumulation in the high pH microenvironments of *Phaeocystis* sp. (Haptophyceae) colonies from the North Sea. *Mar. Ecol. Prog. Ser.* **59**, 285-293.

Lucas A. and Beninger P. G. (1985) The use of physiological condition indices in marine bivalve aquaculture. *Aquaculture* **44**, 187-200.

873 Marigómez I., Soto M., Cajaraville M., P. , Angulo E. and Giamberini L. (2002)
874 Cellular and subcellular distribution of metals in molluscs. *Microsc. Res.*
875 *Techniq.* **56**, 358-392.
876 Markich S., Jeffree R. and Burke P. (2002) Freshwater bivalve shells as archival
877 indicators of metal pollution from a copper-uranium mine in tropical northern
878 Australia. *Environ. Sci. Technol.* **36**, 821-832.
879 Millward G., Morris A. and Tappin A. (1998) Trace metals at two sites in the
880 southern North Sea: Results from a sediment resuspension study. *Cont. Shelf*
881 *Res.* **18**, 1381-1400.
882 Misogianes M. and Chasteen N. (1979) A chemical and spectral characterization of
883 the extrapallial fluid of *Mytilus edulis*. *Anal. Biochem.* **100**, 324-334.
884 Morris A. (1971) Trace metal variations in sea water of the Menai Straits caused by a
885 bloom of *Phaeocystis*. *Nature* **233**, 427-428.
886 Morris A. (1974) Seasonal variation of dissolved metals in inshore waters of the
887 Menai Straits. *Mar. Poll. Bull.*, 54-59.
888 Mucci A. (1988) Manganese uptake during calcite precipitation from seawater:
889 Conditions leading to the formation of pseudokutnahorite. *Geochim.*
890 *Cosmochim. Ac.* **52**, 1859-1868.
891 Mucci A. and Morse J. W. (1990) Chemistry of low-temperature abiotic calcites:
892 experimental studies on coprecipitation, stability and fractionation. *Aquat. Sci.*
893 **3**, 217-254.
894 Nico P., Anastasio C. and Zasoski R. (2002) Rapid photo-oxidation of Mn (II)
895 mediated by humic substances. *Geochim. Cosmochim. Ac.* **66**, 4047-4056.
896 Park H., Ahn I.-Y., Lee J. K., Shin S. C., Lee J. and Choy E.-J. (2009) Molecular
897 cloning, characterization, and the response of manganese superoxide
898 dismutase from the Antarctic bivalve *Laternula elliptica* to PCB exposure.
899 *Fish Shellfish Immun.* **27**, 522-528.
900 Parsons T., Muita Y. and Lalli C. (1984) *A manual of chemical and biological*
901 *methods for seawater analysis*. Pergamon Press, Oxford.
902 Pentreath R. (1973) The accumulation of ^{65}Zn, ^{54}Mn, ^{58}Co and ^{59}Fe by the mussel
903 *Mytilus edulis*. *J. Mar. Biol. Assoc. U.K.* **53**, 127-143.
904 Pieters H., Kluytmans J. H., Zandee D. I. and Cadée G. C. (1980) Tissue composition
905 and reproduction of *Mytilus edulis* in relation to food availability. *Neth. J. Sea*
906 *Res.* **14**, 349-361.
907 Pietrzak J., Bates J. and Scott R. (1976) Constituents of unionid extrepallial fluid. ii
908 pH and metal ion composition. *Hydrobiologia* **50**, 89-93.
909 Pingitore J., Nicholas E., Eastman M., Sandidge M., Oden K. and Freiha B. (1988)
910 The coprecipitation of manganese (II) with calcite: an experimental study.
911 *Mar. Chem.* **25**, 107-120.
912 Poigner H., Monien P., Monien D., Kriews M., Brumsack H.-J., Wilhelms-Dick D.
913 and Abele D. (2013) Influence of the porewater geochemistry on Fe and Mn
914 assimilation in *Laternula elliptica* at King George Island (Antarctica). *Estuar.*
915 *Coast. Shelf S.* **135**, 285-295.
916 Prins M. A., Dankers N. and Smaal A. C. (1994) Seasonal variation in the filtration
917 rates of a semi-natural mussel bed in relation to seston composition. *J. Exp.*
918 *Mar. Biol. Ecol.* **176**, 69-86.
919 Richardson C. (2001) Molluscs as archives of environmental change. *Oceanogr. Mar.*
920 *Biol.* **39**, 103-164.

Richardson L., Aguilar C. and Nealson K. (1988) Manganese oxidation in pH and O_2 microenvironments produced by phytoplankton. *Limnol. Oceanogr.* **33**, 352-363.

Richardson L. and Stolzenbach K. (1995) Phytoplankton cell size and the development of microenvironments. *FEMS Microbiol. Ecol.* **16**, 185-192.

Roitz J., Flegal A. and Bruland K. (2002) The biogeochemical cycling of manganese in San Francisco Bay: Temporal and spatial variations in surface water concentrations. *Estuar. Coast. Shelf S.* **54**, 227-239.

Schlitzer R. (2014) Ocean Data View. http://odv.awi.de.

Schoemann V., de Baar H., de Jong J. and Lancelot C. (1998) Effects of phytoplankton blooms on the cycling of manganese and iron in coastal waters. *Limnol. Oceanogr.* **43**, 1427-1441.

Seed R. and Suchanek T. (1992) Population and community ecology of *Mytilus*. In *The mussel Mytilus: Ecology, Physiology, Genetics and Culture* (ed. E. Gossling). Elsevier, Amsterdam. pp. 87-170.

Simkiss K. and Mason A. (1983) Metal Ions: Metabolic and toxic effects. In *The Mollusca* (ed. P. W. Hochachka). Academic Press, New York. pp. 102-164.

Simkiss K. and Mason A. Z. (1984) Cellular responses of molluscan tissues to environmental metals. *Mar. Environ. Res.* **14**, 103-118.

Smaal A. C. and Twisk F. (1997) Filtration and absorption of *Phaeocystis* cf. *globosa* by the mussel *Mytilus edulis* L. *J. Exp. Mar. Biol. Ecol.* **209**, 33-46.

Smaal A. C., Vonck A. P. M. A. and Bakker M. (1997) Seasonal Variation in Physiological Energetics of *Mytilus edulis* and *Cerastoderma edule* of Different Size Classes. *J. Mar. Biol. Assoc. U.K.* **77**, 817-838.

Su P. and Huang S. (1998) Direct and simultaneous determination of copper and manganese in seawater with a multielement graphite furnace atomic absorption spectrometer. *Spectrochim. Acta B* **53**, 699-708.

Sunda W. and Huntsman S. (1985) Regulation of cellular manganese and manganese transport rates in unicellular alga *Chlamydomonas*. *Limnol. Oceanogr.* **30**, 71-80.

Sunda W. and Huntsman S. (1987) Microbial oxidation of manganese in a North Carolina Estuary. *Limnol. Oceanogr.* **32**, 552-564.

Sundby B., Anderson L., Hall P., Iverfeldt A., Rutgers V., Der Loeff M. and Westerlund S. (1986) The effect of oxygen on release and uptake of cobalt, manganese, iron and phosphate at the sediment-water interface. *Geochim. Cosmochim. Ac.* **50**, 1281-1288.

Turner A. and Millward G. (2000) Particle dynamics and trace metal reactivity in estuarine plumes. *Estuar. Coast. Shelf S.* **50**, 761-774.

Vander Putten E., Dehairs F., Keppens E. and Baeyens W. (2000) High resolution distribution of trace elements in the calcite shell layer of modern *Mytilus edulis*: Environmental and biological controls. *Geochim. Cosmochim. Ac.* **64**, 997-1011.

Wada K. and Fujinuki T. (1976) Biomineralization in bivalve molusca with emphasis on the chemical composition of extrapallial fluid. In *The Mechanisms of Mineralization in the Invertebrates and Plants* (eds. N. Watabe and K. M. Wilbur). Univ. of South Carolina Press, Columbia. pp. 175-188.

Wang W.-X. and Rainbow P. S. (2008) Comparative approaches to understand metal bioaccumulation in aquatic animals. *Comp. Biochem. Phys. C* **148**, 315-323.

969 Widmeyer J. R., Crozier E. D., Moore M. M., Jurgensen A. and Bendell-Young L. I.
970 (2004) Role of *Leptothrix discophora* in mediating metal uptake in the filter-
971 feeding bivalve *Mytilus trossulus* (*edulis*). *Environ. Sci. Technol.* **38**, 769-774.
972 Wilbur D. and Saleuddin A. (1983) Shell formation. In *The Mollusca* (eds. A. S. M.
973 Saleuddin and K. M. Wilbur). Academic Press, New York. pp. 236-287.
974 Yin Y., Huang J., Paine M., Reinhold V. and Chasteen N. (2005) Structural
975 characterization of the major extrapallial fluid protein of the mollusc *Mytilus*
976 *edulis*: Implications for function. *Biochemistry* **44**, 10720-10731.
977
978
979
980

Figure Captions

Figure 1. Map with the location of the experimental site (red dot), the Menai Strait, North Wales, United Kingdom (produced with ODV by Schlitzer, 2014).

Figure 2. Seasonal variation of environmental conditions during the field culturing experiment: a) Seawater temperature; b) Salinity; c) Chlorophyll-*a* concentration; d) pH; e) Dissolved inorganic phosphorus, nitrate + nitrite, and silicate concentrations. Letters indicate calendar months.

Figure 3. Seasonal variation of: a) Seawater particulate (Mn_{Part}) and dissolved Mn^{2+} (Mn_{Diss}) concentrations; b)D_{Mn}, the Mn partition coefficient between shell calcite and seawater dissolved Mn, scale is inverted for clarity and seawater dissolved Mn/Ca (mmol/mol); c) Shell Mn/Ca ratios of short- and annual-deployed shells (see text for a detailed description). Horizontal bars indicate the temporal resolution of each shell Mn/Ca sample. Letters indicate calendar months.

Figure 4. Seasonal variation of: a) Tissue dry weight (TDW) and Condition Index (CI); b) Absolute respiration rate (ARR) and weight specific respiration rate (WSRR); c) Shell growth rate (SGR); and d) Shell Mn/Ca ratios of short- and annual-deployed shells (see text for a detailed description). For a) and b) lines are the mean values; symbols are individual data points for each growth interval. Letters indicate calendar months.

Figure 1

Click here to download high resolution image

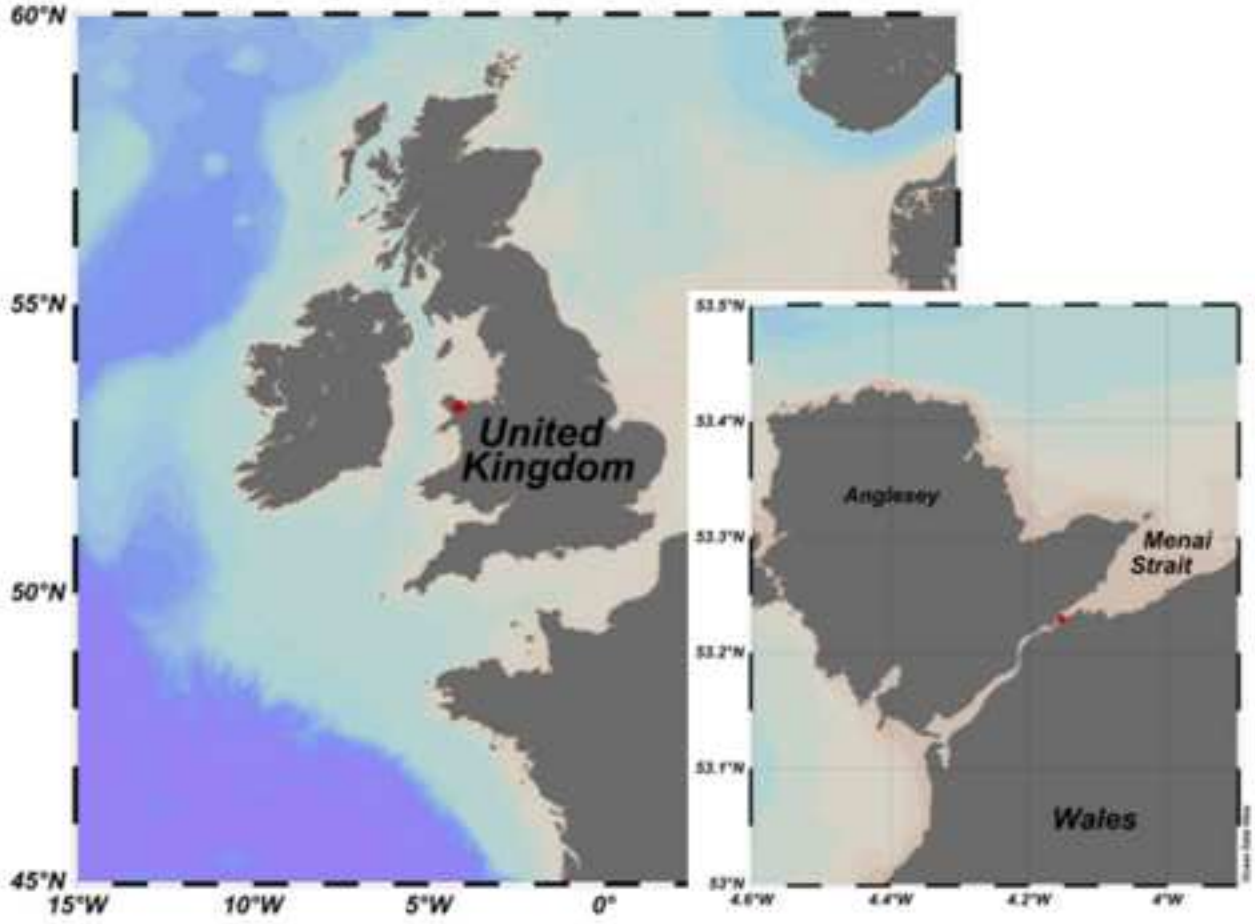

Figure 2

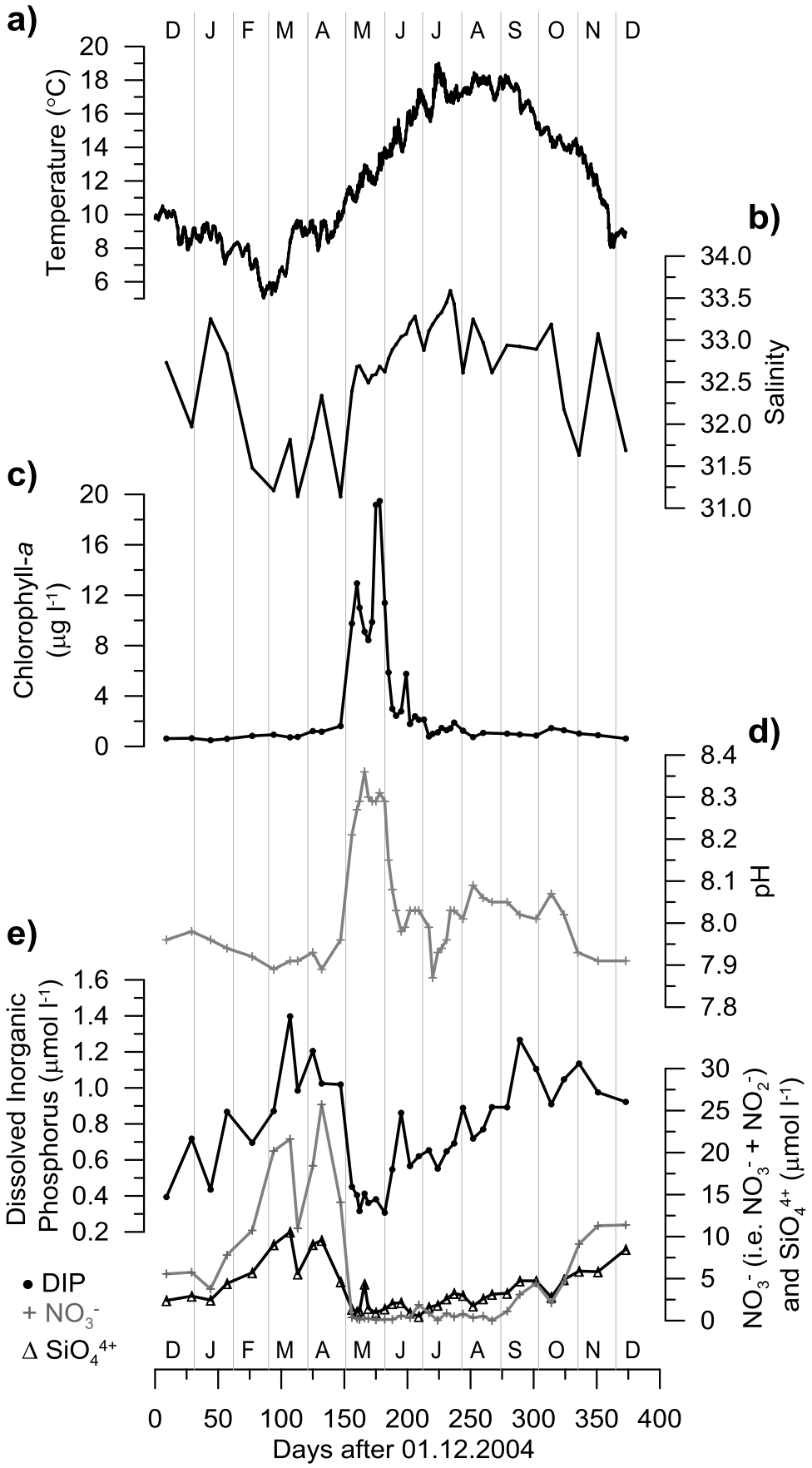
a)
D J F M A M J J A S O N D
Temperature (°C)
20 18 16 14 12 10 8 6
b)
Salinity
34.0 33.5 33.0 32.5 32.0 31.5 31.0
c)
Chlorophyll-a (µg l-1)
20 16 12 8 4 0
d)
pH
8.4 8.3 8.2 8.1 8.0 7.9 7.8
e)
Dissolved Inorganic Phosphorus (µmol l-1)
1.6 1.4 1.2 1.0 0.8 0.6 0.4 0.2
• DIP
+ NO3-
Δ SiO44+
NO3- (i.e. NO3- + NO2-) and SiO44+ (µmol l-1)
30 25 20 15 10 5 0
D J F M A M J J A S O N D
0 50 100 150 200 250 300 350 400
Days after 01.12.2004

Figure 3

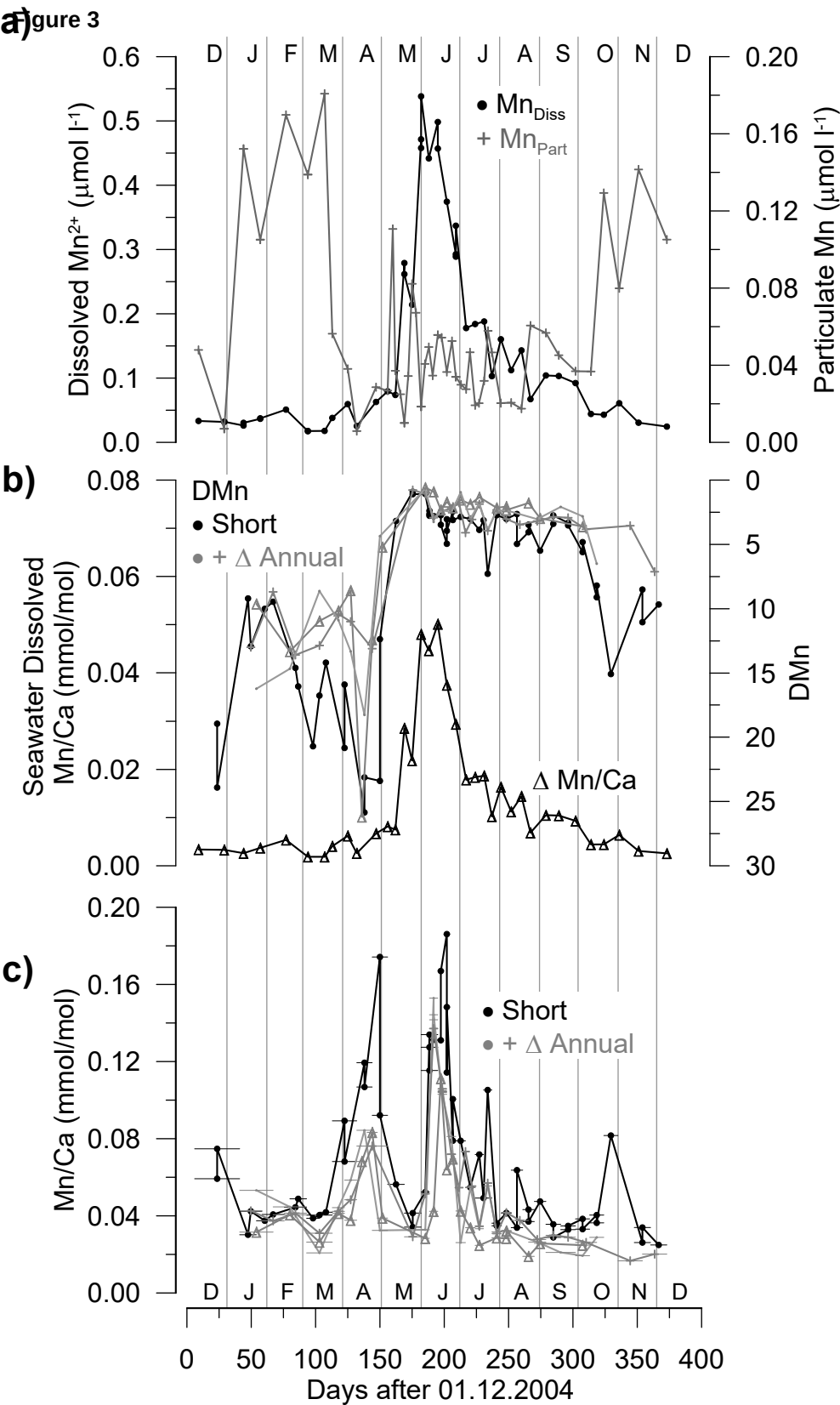
a)
b)
c)
D J F M A M J J A S O N D
Dissolved Mn2+ (µmol l-1)
Particulate Mn (µmol l-1)
MnDiss
+ MnPart
Seawater Dissolved Mn/Ca (mmol/mol)
DMn
Short
+ Δ Annual
Δ Mn/Ca
Mn/Ca (mmol/mol)
0 50 100 150 200 250 300 350 400
Days after 01.12.2004

Figure 4

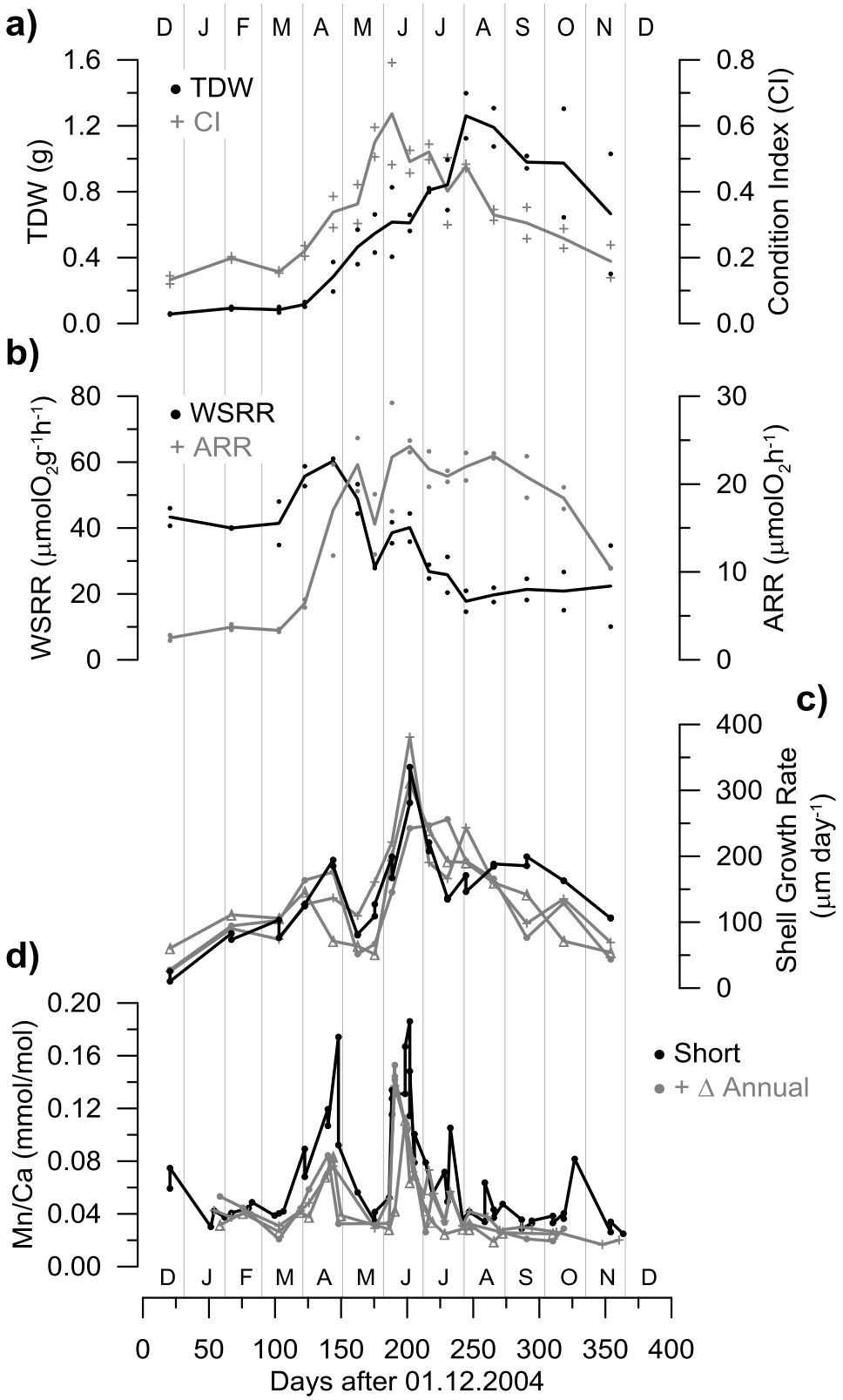
a)
D J F M A M J J A S O N D
TDW
CI
TDW (g)
Condition Index (CI)
b)
WSRR
ARR
WSRR (µmolO2g-1h-1)
ARR (µmolO2h-1)
c)
Shell Growth Rate (µm day-1)
d)
Mn/Ca (mmol/mol)
Short
+ Δ Annual
Days after 01.12.2004